SSRG International Journal of Electrical and Electronics Engineering
ISSN: 2348-8379 / https://doi.org/10.14445/23488379/IJEEE-V10I2P113

Volume 10 Issue 2, 132-142, February 2023
© 2023 Seventh Sense Research Group®

Original Article

Substantiation of Requirements to the Gas Discharge Visualization-Based Technical System for Studying Bio-objects

Natalia Kosulina[1], Stanislav Kosulin[2], Kostiantyn Korshunov[3], Mykola Lysychenko[4], Maksym Sorokin[5], Yuri Handola[6], Huzenko Vitalii[7]

[1,3,4,5,6,7]*Department of Electromechanics, Robotics, Biomedical and Electrical Engineering. State Biotechnological University.*
[2]*Department of Oncosurgery Radiation Therapy and Palliative Care, Kharkiv Medical Academy of Postgraduate Education, Kharkiv, Ukraine.*

[1]*Corresponding Author: kosnatgen@ukr.net*

Received: 10 January 2023 Revised: 08 February 2023 Accepted: 19 February 2023 Published: 28 February 2023

Abstract *- The article presents the requirements substantiation for a technical system based on gas-discharge visualization used to study biological objects. The following was considered: grounding and choice of the method for generating high-voltage pulse signals for biological objects gas-discharge visualization; the formation of synchronizing impulses and time intervals; the device for amplitude stabilization of impulses in the generator for biological objects gas-discharge visualization; requirements for the key of the pulse generator and the pulse transformer justification; substantiation and selection of the functional diagram of the power supply.*

Keywords *- Biological object, Gas discharge visualization, Technical system.*

1. Introduction

The control system for studying biological objects being under the influence of EMR is very diverse in its purpose, types of applied exposures, construction principles, and complexity.

Yet, despite this, it is possible to compile its generalized description, which allows us to consider the essence of the problems arising during the construction of a system for monitoring biological objects. Such a description should include the definition of a biological object's control system and the structural diagram assignment in a form that allows studying its organization's morphological, functional and informational aspects.

Rational engineering of a biological object's control system for the study is impossible without measuring the beneficial effect caused by the influence on a biological object. This circumstance dictates the need to use a systematic approach in order to study engineering system problems in the study of biological objects.

The systems approach requires a biological object to be considered an integral part of the biological object control system. In this case, the functioning of the "bio-object - technical devices" complex is formed. The design and engineering of a bio-objects monitoring system should ensure a certain efficiency of this complex.

2. Literature Review and Problem Statement

In research [5,6], a system classification distinguishing physical, technical, cybernetic, biological, social and intellectual systems as the main classes is proposed. Physical, technical, and cybernetic systems differ in the level of organization and the ability to adapt to new operating conditions. Depending on the complexity of the structure and internal relationships organization, the control system for the biological objects study can be defined as a biophysical, biotechnical or biocybernetics system. It should be noted that some internal environment through which the biological object is affected forms in the biological object's control system. The internal environment designates a scalar or vector field of certain physical factors (thermal, electromagnetic, sound, etc.), purposefully organized and controlled in the local part of the space surrounding the biological object.

The control of the internal environment parameters is carried out by the technical part of the system, consisting of actuators that regulate the access of matter or energy to the internal environment, thereby organizing influences V; a control device designed to generate signals controlling actuators; a master device designed to set the required process indicators, which are controlled in the system; in a particular case, it forms a given program of influence on a biological object; a device for measuring and processing information about a biological object and the internal environment of the system, necessary for analyzing the state of the object, controlling and generating information signals S. The system interacts with the external environment. The external environment of the system is a source of matter, energy, and disturbances that affect its functioning. Connections between the elements of the generalized scheme indicate the direction of the transfer of information and matter-energy influences in the system.

So, in the most complex type of a biotechnical system, self-organization can be applied in it. This means that information about the current state of the internal environment and the biological object should be used to find means of control optimal for the current state yet able to emerge the effect that satisfies the specified criterion at the end of the functioning process. In a simpler biotechnical system type, the process can be controlled according to a set program for changing the parameters of the internal environment or a biological object. Such control is possible both in a closed system (with feedback) and an open one. Naturally, in a closed system, a higher quality of control can be achieved with variations in the system parameters and the action of disturbances from the external environment [7, 8].

Considering these principles in [5–8] makes it possible to single out interrelated problems that have independent significance in constructing a control system for the study of biological objects. These requirements include: modeling the structure of functions and properties of biomaterials that change under the influence of factors in the internal environment of the system; development of methods for processing information about the state of biological objects; allowing to organize the management of impacts on biological objects; modeling of the system (processes) for controlling the physical factors of the internal environment; assessment of the effectiveness of the biological object control system; selection (justification) and coordination of technical requirements for the biological objects` control system for studying biological objects under the influence of an electromagnetic field (EMF).

With all the variety of specific theoretical solutions [6], the essence of the gas discharge visualization (GDV) process can be reduced to a certain theoretical scheme.

The primary process is the process of interaction between impulse voltage and the object of study that, under a certain electric field strength, creates an emission of charged particles that are radiated by the object`s surface, involved in the initiation of the initial phases of the gas discharge. The gas discharge, in turn, can affect the object's state, causing secondary emission, destructive and thermal processes. Thus, in the process of GDV, a certain sequence of information transformations is formed. The state of a biological object is characterized by physiological processes and biological indicators, among which the determining role, from the GDV point of view, are physicochemical and emission processes, as well as gas emission processes, which depend on the parameters of the exposure on the biological object (seeds of agricultural crops) of EMF EHF range [10, 11].

The parameters of the gas discharge vary due to the inhomogeneity of the surface and volume, the processes of emission of charged particles affecting the high-voltage parameters, leading to the change of gas-discharge parameters. These parameters are the characteristics of the discharge current and optical radiation. In this case, the radiation receiver converts the spatial distribution of brightness into an image, and the analysis of the amplitude characteristics of the video signals leads to forming of a set of parameters. During performed studies, it was noticed that the GDV-gram shows a complex of parameters and features of the biological object, related both with the processes of homeostasis of the whole organism and with local electrical phenomena. In other words, the bio-object information extraction occurs due to processes of several levels: the bio-object is put in the electric current circuit in the system of connected LC circuits, and therefore changes in the complex resistance of the bio-object due to physiological processes lead to a redistribution of currents in the circuit and change the parameters of the gas discharge; a biological object is an object with a non-uniform distribution of elements with different conductivity near the surface. This leads to the formation of an inhomogeneous voltage distribution near the surface, which affects the nature of the discharge development; the nature of the image and the process of development of the discharge depends not only on the structural organization of the biological object but also on the parameters of the voltage pulse: pulses duration; the number of pulses in a pulse burst; the peak of the top of the pulse; pulse duration errors; pulse increase and drop duration; pulse instability repetition rate; pulse repetition period.

In most cases, as shown in article [12], the formed image is the result of the combined action of two processes. First, an avalanche discharge develops in a narrow gap limited by the dielectric surfaces of the biological object and the image carrier. Under certain conditions, this process can initiate a sliding discharge over the dielectric surface. In the process of GDV, a complex interaction between a biological object and an applied impulse voltage is carried out. In the GDV process, due to the applied impulse voltage and gas discharge excitation, information about the parameters of the studied biological object is converted into information about the characteristics of the gas discharge image.

From the point of view of quantum theory, the impulse voltage is a quantum amplifier for biological object radiation, which can induce the information-polarized EMF of the EHF range. Suppose radical reactions are maintained in the biological object, which reflects the metabolism and the functioning of the processes of forming free radicals. In that case, the obtained GDV-grams will carry information about the parameters of the EMF affecting the biological object [13, 14].

Theoretical studies and analysis of existing GDV devices have shown that for the study of biological objects for agricultural purposes (soybean seeds), pulse generators are needed that meet the following requirements: pulse voltage amplitude 15…20 kV; pulse duration 10^{-6} s; the number of pulses in a pack of 100 pcs.; the pulse peak slope not more than 0,005U; the error of the pulse repetition period is not more than $10^{-4}T_1$; pulse duration error no more than $\pm 0{,}01\,\tau$; pulse front duration 10 ns; pulse cutoff duration 20 ns; pulse repetition period $T_1=1/f_1=10^{-5}$; repetition period of a burst of pulses $T_2=1/f_2=10^{-3}$ s [15, 16, 17].

The purpose of the study is to substantiate the technical system requirements for the study of biological objects based on gas-discharge visualization.

To achieve the goal, the following tasks were set:

- substantiation and choice of a method for generating high-voltage pulse signals for biological objects gas-discharge visualization;
- the formation of synchronizing pulses and time intervals;
- a device for amplitude stabilization of pulses in the generator for gas-discharge visualization of biological objects;
- justification of the requirements for the switch of the pulse generator and the pulse transformer;
- substantiation and choice of the functional scheme of the power supply.

3. Materials and Methods

For the formation of high-voltage pulse signals with a duration, $\tau = 10^{-6}$two main methods have been used.

The first is to amplify low-power pulses to the required value; the second method is to control a high-voltage source of the required power, which is switched on for the pulse duration by the switching device.

On fig. 1 shows a functional diagram of a generator for biological objects GDV.

The scheme includes: 1 – generator of synchronizing pulses (frequency 100 kHz); 2 – registration time generator; 3,4,5 – switches; 6 – synchronization pulse shaper; 7 – shaper of the duration of a burst of pulses; 8 – pause shaper; 9 – the device for amplitude stabilization of current pulses in the transformer; 10 – power amplifier; 11 – current switch; 12 – network filter; 13 – power supply of the charging capacity; 14 – service power supply; *D1* – *RS* trigger.

The functional diagram (Fig. 1) is based on the method of accumulating electrical energy in the form of a magnetic field energy of a certain inductance (magnetic storage). Magnetic storage has a significant advantage over other storage (capacitive, artificial line).

The advantage of a magnetic storage device is that, with a relatively small mass and dimensions, it allows the accumulation of significant energy.

The operation of the magnetic storage is controlled by a power current switch, which, in turn, is controlled by a shaper and a device for pulse amplitude stabilization. The use of the shaper is due to the need to generate a required waveform and power signal from a low-power synchronization pulse.

To stabilize the amplitude of the output pulse, a tracking system for stabilizing the maximum current of the magnetic storage charge was used.

Using a tracking autoregulation system makes it possible to obtain a high accuracy of pulse amplitude track – less than 1%. Stabilization of the amplitude of the pulses is carried out by the action of the servo stabilization system on the current switch.

The scheme of time intervals and synchronizing pulses formation is shown in fig. 2.

This scheme generates a registration time interval of 10 s, a burst duration interval of 10^{-3} s, a pause between pulse bursts of 10^{-2} s, and a synchronization pulse duration of 5 µs.

A quartz clock generator generates pulses with a frequency of 100 kHz. Further, these pulses flow to the *K1* switch and to the synchronization pulse shaper; simultaneously, a registration time pulse equal to 10 s is applied to *K1*. The synchronization pulse shaper generates a pulse with a duration of 1 µs, which flows to the *K2* switch. The second input of the *K2* switch receives a pulse from the *K1* switch. From the output of the *K2* switch, a pulse with a duration of 1 µs flows to the input of the *K3* switch, and a signal allowing the passage of a burst of pulses, or a pause signal, is sent to the second input of the *K3* switch. The burst pulses duration shaper through the RS-trigger turns on *K3*, and the pause shaper through the RS-trigger turns off the *K3* switch; from the output of *K3*, the signal enters the logic device.

After 10 s, the signal from the registration time generator prohibits the passage of 100 kHz pulses, locking the *K1* switch.

To resume the shaper, you must press the SB button. The clock generator scheme provides increased frequency stability over a wide range of ambient temperatures. The generator pulse frequency and stability are set by the parameters of the quartz resonator [18]. The clock pulse generator can be constructed on SN7400 microcircuits.

To stabilize the frequency of the registration time generator, clock quartz at a frequency of 32168 Hz can be used.

The burst and pause shaper is a digital multivibrator that generates precise time intervals of impulses and pauses. The time interval shaper can be made on microcircuits of the 561 series: *D1*…*D5* – CD4017A, *D6* – CD4011.

The stabilization circuit maintains the current amplitude in the primary winding of the pulse transformer at a given level (Fig. 3).

The amplitude of each pulse is set depending on the amplitude of the current of the pulse that precedes it so that the difference between the given level and the level of the previous pulse is minimal.

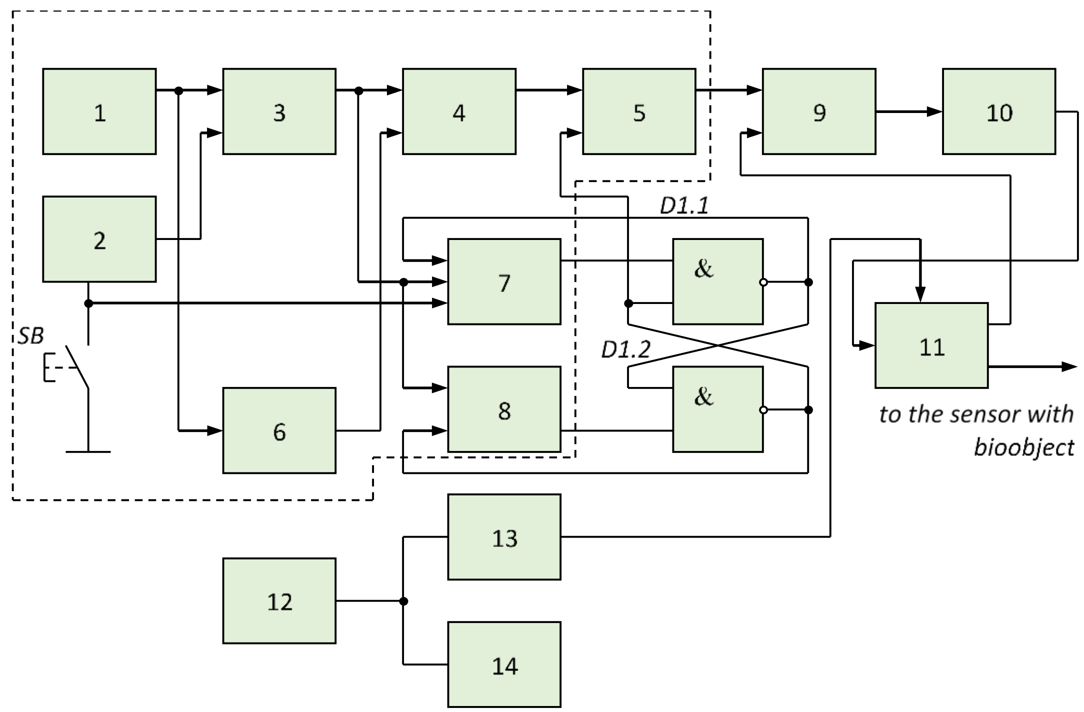

Fig. 1 Functional diagram of the high-voltage pulse generator

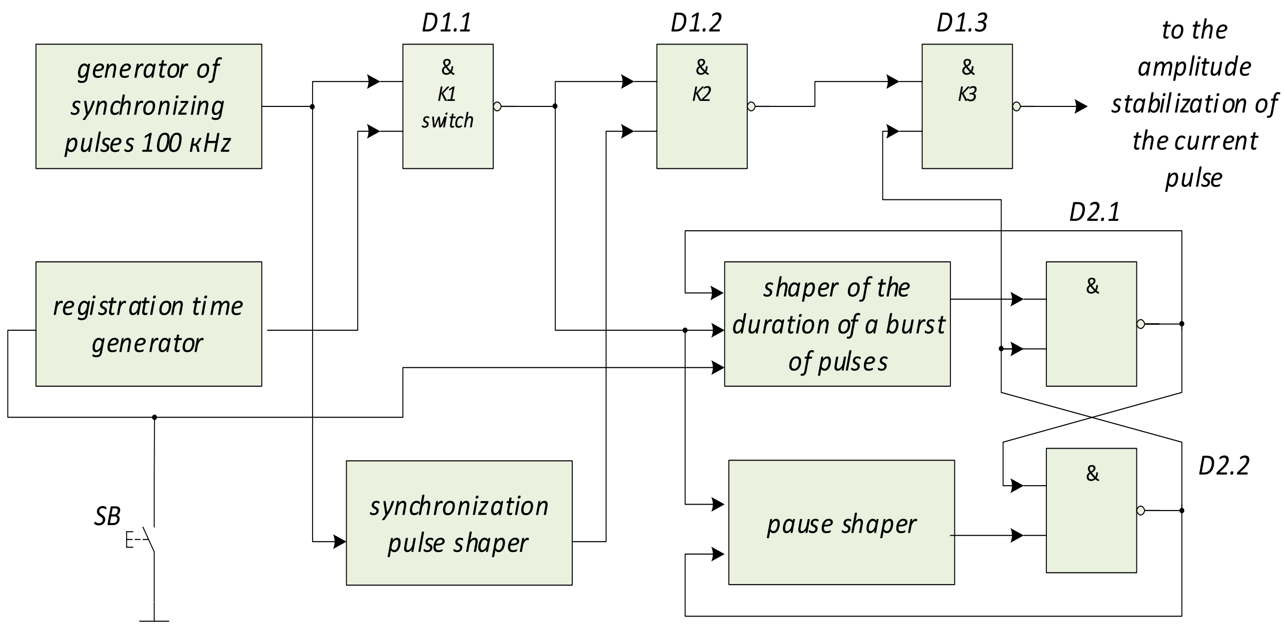

Fig. 2 Functional scheme of the synchronizing pulses and time intervals formation

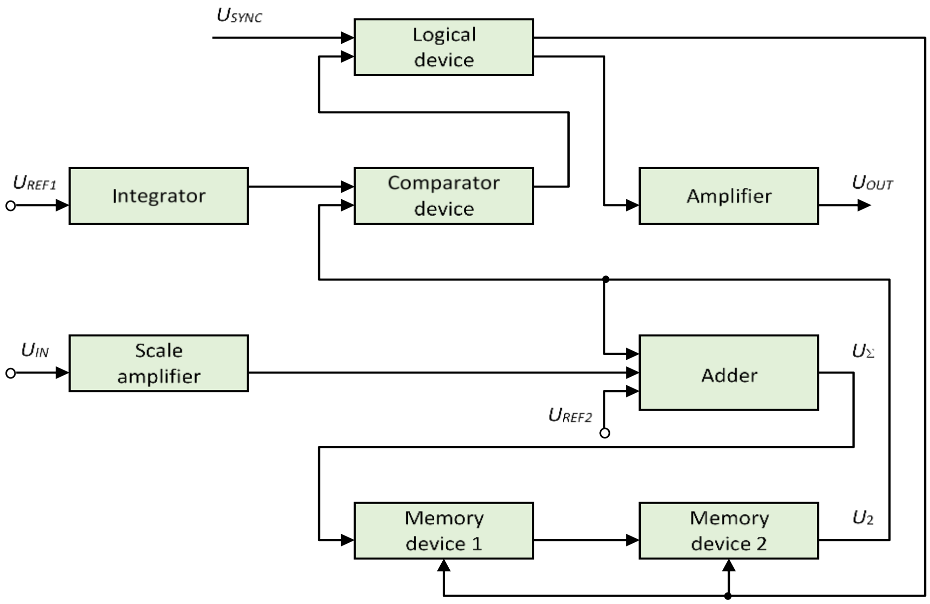

Fig. 3 Functional pulses amplitude stabilization device diagram

The input signal U_{IN}, which is proportional to the amplitude of the pulse transformer's primary winding current, passes through the scaling amplifier and enters the input of the adder. At the output of the adder, we obtain the algebraic sum of the voltages:

$$U_{\Sigma} = kU_{IN} + (-U_{REF2}) + U_2, \quad (1)$$

where k is the scale amplifier factor (gain factor); U_{IN} – input voltage from the current sensor; U_2 – is the voltage recorded on the adder; U_{REF2} – reference voltage.

The sum of the voltages U_{Σ} flows through the memory devices 1 and 2 to the comparator, the reference for the comparator. When the voltage coming from the integrator reaches level U_2, the comparing device will change its state, and the amplifier will turn on the power switch.

A change in reference voltage U_2 leads to a change at the moment when the output switch is turned on and, therefore, the time during which the pulse transformer is connected to the power source changes.

Since the pulse transformer is an integrating link, the current amplitude at the end of the period will be proportional to the time during which the power switch is on, therefore, proportional to the voltage U_2. The following process will continue until U_{Δ} (increment U_2) becomes close to zero. After that, U_2 will stop changing, and the current amplitude in the pulse transformer will be fixed at a certain level.

The D1.1 element inverts the input clock pulses and through one of the open switches (*D2.3* or *D2.4*) starts the shaper, constructed on the elements *D3.1* and *D3.2*, and the shaper on the elements *D3.2* and *D3.4*. The duration of pulses from these shapers is 12 µs, i.e., exceeds the input clock cycle. The "OR" circuit on the *D4.1* elements includes the switch *D4.2* if at least one of the shapers is running.

RS-trigger is constructed on the *D4* chip (CD4027BE), which records the triggering of the comparing device. If the *D4.2* switch opens, the RS trigger turns on the power amplifier. If the time after the arrival of the last clock pulse exceeds 12 µs, then the *D4.2* switch will close, and regardless of the state of the RS-trigger, the power amplifier will turn off the power switch.

The power current switch is designed to control the magnetic storage device and to obtain the required shape and power of pulse signals. It can consist of preliminary and output stages (Fig. 5).

The output stage of the current switch is constructed on a BV2310 field-effect transistor, the capacity of which is a pulse transformer. The preliminary stage is made on a bipolar transistor 2N4235 with a transformer capacity, one of the windings of which is demagnetizing.

The operation of the magnetic storage device is controlled by a current switch, which, in turn, is controlled by a preliminary stage on a bipolar transistor and an amplitude stabilization device. The presence of the previous cascades is due to the need to obtain a signal of the required shape and power obtained from the synchronization pulse [19–21].

The pulse transformer is used to increase the voltage of the pulses and to decouple the potentials of the transformer's secondary circuit from the supply circuit's potential, as well as to eliminate the direct current component of the supply source in the load.

For GDV, the main requirement for a pulse transformer is the undistorted transfer of the shape of the transformed voltage pulses.

For the short voltage pulse transformation, we mostly use transformers of a special design with a ferromagnetic core based on the principle of electromagnetic induction.

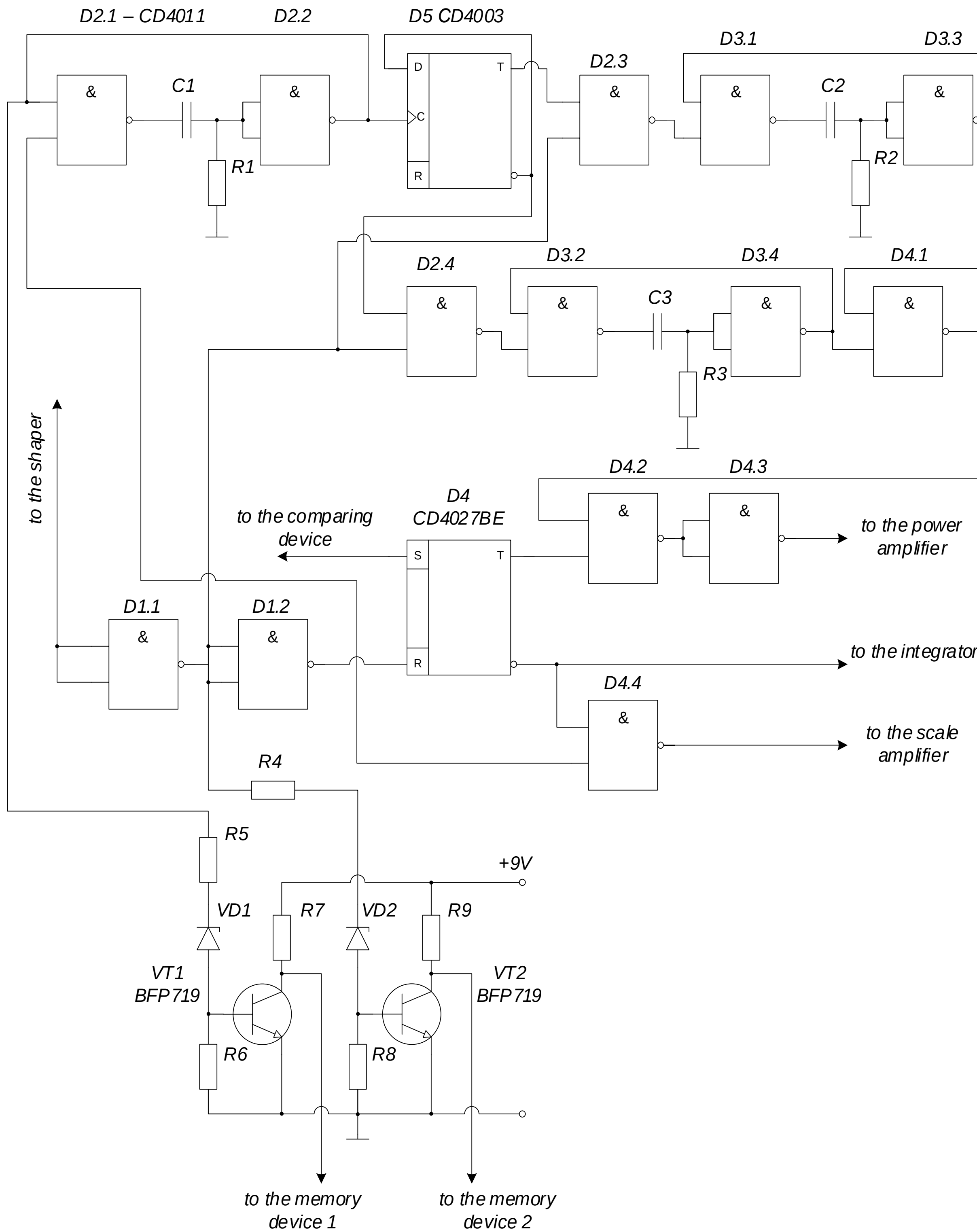

Fig. 4 Electrical diagram of the logic device

With regard to the undistorted transmission of the transformed pulse shape, the main and decisive importance that determines the design and dimensions of the pulse transformer is the parasitic oscillatory processes that occur in the transformer circuit. These processes are mainly caused by the transformer windings' parasitic capacitance and leakage inductance. Oscillatory processes lead to distortion of the front and cutoff of the transformed pulses.

To eliminate the distortion of the shape of the transformed pulse, striving for the parasitic parameters' magnitude reduction is necessary. This is achieved using a core made of special magnetic alloys and windings of the required design. However, the main importance in this direction is to reduce the size of the core and the number of turns of the windings.

Decreasing following values leads to a rapid rate of change increase in the induction in the core, which reaches colossal values, reaching up to 100 T per second, significantly exceeding the rate of induction change in conventional low-frequency transformers. At such rates of induction change, powerful eddy currents are induced in the mass of the core, which, if the design is incorrect, can lead to unacceptable distortion of the pulse top.

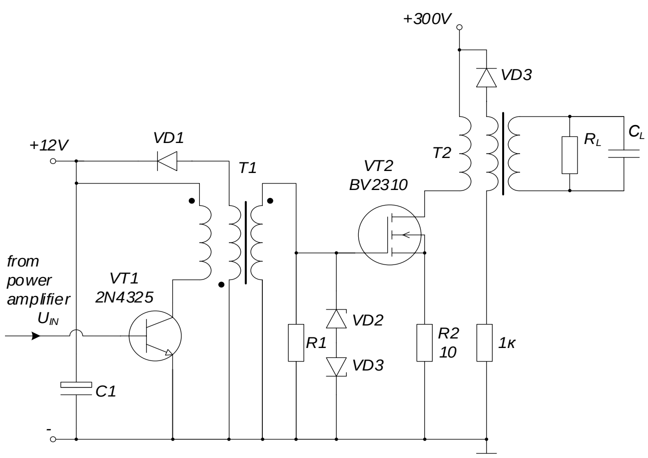

Fig. 5 Electrical circuit of the current switch

The overall picture of the processes in the core is determined by the following main physical phenomena:

- The phenomenon of electromagnetic induction, which establishes a relationship between the voltage applied to the transformer winding and the law of change in magnetic flux in the core;
- The phenomenon of hysteresis determines the relationship between the magnitude of the magnetic induction in the core and the magnetizing current;
- The phenomenon of magnetic aftereffect due to the specific inertial properties of magnetic materials (magnetic viscosity), which manifests itself in the time delay of the magnetization of the material relative to the magnetizing current.

4. Results and Discussion

The listed phenomena determine the processes in the transformer`s core in any mode of operation. However, in the pulse mode, the significance and effect of some of these phenomena become especially significant. In addition, the nature of the processes caused by the hysteresis phenomenon takes on specific forms in the pulse mode.

When considering the processes in the core, in order to simplify the analysis, we will assume that the active resistances of the windings, their leakage inductance and the parasitic capacitances of the windings and loads are equal to zero. These parameters have little effect on the processes in the "hardware" of the transformer.

Let us condition the use of a generator of rectangular pulses (Fig. 6), which generates a pulse with amplitude $U_T=E$ and τ duration. The output impedance of the generator is R_i. The generator outputs are connected to the input terminals of the primary winding *1-1* of the pulse transformer *Tr*.

The secondary winding of the transformer is loaded with the resistor R_L and capacitance C_L. It is required to determine the shape of the output pulse at the output terminals of the transformer 2-2 and evaluate the pulse shape distortion during transmission.

To solve the problem, we recalculate the load elements in the transformer's primary winding circuit to points *2′-2′* and determine the voltage between these points. Then, using the transformation ratio *n*, calculate the output voltage between points *2-2* by proportional recalculation.

Using the equivalent circuit of the transformer, as well as the ratios for recalculating the load elements $R_2=R_L/K_{Tr}^2$, $C=K_{Tr}^2 C_L$ and the transmission circuit diagram, can go to the form (Fig. 7) [22–24], where L_S is the leakage inductance of the transformer; L_M is the magnetizing inductance of the transformer; K_{Tr} – voltage transformation ratio.

The scheme obtained after such a replacement (Fig. 7) contains three independent reactive energy storage devices: L_S, L_M, and C_L. Therefore, it is described by a third-order differential equation.

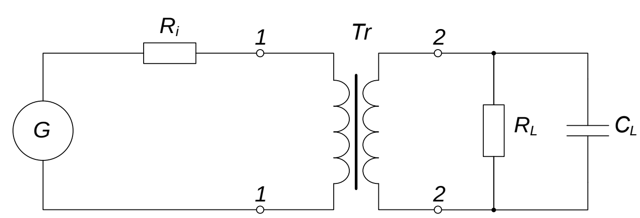

Fig. 6 Electric circuit of the rectangular pulses generator

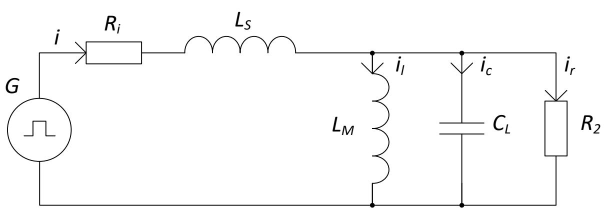

Fig. 7 Generator equivalent circuit

If, by the beginning of the impact of the input voltage pulse (t=0), the transformer circuit is usually free of initial energy reserves, i.e. $i(0)=0$ и $U_{IN}(0)=0$, then under these initial conditions, the transient processes in the circuit (Fig. 7) will be described by the equation:

$$E=\frac{R_i}{L_M}\int_0^{\tau_u}u(t)\,dt+\frac{R_i}{R_2}u(t)+$$

$$+R_iC\frac{du(t)}{dt}+\frac{L_S}{L_M}u(t)+$$

$$+\frac{L_S}{R_2}\frac{du(t)}{dt}+L_SC\frac{d^2u(t)}{dt^2}+u(t). \quad (2)$$

Assuming, $U(t)\to U(p)$.

Then for zero initial conditions:

$u'(t)\to pu(p)$;

$u''(t)\to p^2u(p)$;

$\int_0^{\tau_u}u(t)dt\to\frac{1}{p}u(p)$.

The constant E has an image E/P. In an operator form, equation (2) can be written in the following form:

$$\frac{E}{p}=\frac{R_i}{L_M}\frac{1}{p}U(p)+\frac{R_i}{R_2}U(p)+R_i\cdot C\cdot pU(p)+$$

$$+\frac{L_S}{L_M}U(p)+\frac{L_S}{R_2}pU(p)+L_SCp^2U(p)+U(p). \quad (3)$$

From equation (3), we get:

$$U(p)=\frac{E\cdot\frac{1}{L_SC}}{p^3+\left(\frac{R_i}{L_S}+E\cdot\frac{1}{R_2C}\right)p^2+\left(\frac{R_i}{R_2}+\frac{L_S}{L_M}+1\right)\frac{1}{L_SC}p+\frac{R_i}{L_M}\frac{1}{L_SC}}; \quad (4)$$

$a(p)=E\cdot\frac{1}{L_SC}=a_0=const$;

$b(p)=p^3+rp^2+sp+\psi$;

where:

$$r=\frac{R_i}{L_S}+\frac{1}{R_2C};$$

$s=\left(\frac{R_i}{R_2}+\frac{L_S}{L_M}+1\right)\frac{1}{L_SC}$;

$\psi=\frac{R_i}{L_M}\cdot\frac{1}{L_SC}$.

To find the roots of the polynomial in equation (4), we will replace the unknown $y=p+(r/3)$ and obtain the so-called reduced equation:

$$y^3+my+q=0, \quad (5)$$

where:

$m=\frac{3s-r^2}{3}$;

$q=\frac{2r^3}{27}-\frac{rs}{3}+\psi$.

Depending on m sign and discriminant D:

$$D=\left(\frac{m}{3}\right)^3+\left(\frac{q}{2}\right)^2, \quad (6)$$

The transient process will be aperiodic, critical or oscillatory in its essence. In the first case, it is necessary that $m<0$ и $D<0$. In the second case, it is necessary that $m<0$ и $D=0$. During the oscillatory process, the conditions are $m<0$ и $D>0$.

We will consider the critical mode to execute the conditions associated with the requirements for the GDV pulse parameters.

For the critical mode, the value of the roots for equation (5) will be determined by the expressions [23]:

$y_1=-2R\cos\frac{\phi}{3}$;

$y_2=-2R\cos\left(\frac{\phi}{3}+\frac{2\pi}{3}\right)$;

$$y_3=-2R\cos\left(\frac{\phi}{3}+\frac{4\pi}{3}\right), \quad (7)$$

where:

$R=(sign\ g)\frac{\sqrt{|m|}}{3}$;

$\cos\phi=\frac{q}{2R^3}$.

Therefore, the roots of equation (4) will look like this:

$p_1=y_1-\left(\frac{r}{3}\right)$;

$p_2=y_2-\left(\frac{r}{3}\right)$;

$$p_3=y_3-\left(\frac{r}{3}\right). \quad (8)$$

Thus, knowing the representation of the function $U(p)$, we can pass to the original of the desired function using the inverse Laplace transform [9]:

$$U(t)=A_1e^{p_1t}+A_2e^{p_2t}+A_3e^{p_3t}, \quad (9)$$

where:

$A_1=\frac{E\cdot\frac{1}{L_S\cdot C}}{3p_1^2+2rp_1+s}$;

$A_2=\frac{E\cdot\frac{1}{L_S\cdot C}}{3p_2^2+2rp_2+s}$;

$$A_3 = \frac{E \cdot \frac{1}{L_S \cdot C}}{3p_3^2 + 2rp_3 + s}.$$

For the critical mode, the duration of the leading edge of the output pulse is determined from the expression [24]:

$$\tau_F = 2\sqrt{k_D L_S C}, \quad (10)$$

where: $k_D = \frac{1}{L_S C}\left(\frac{1}{3p_1^2+2rp_1+s} + \frac{1}{3p_2^2+2rp_2+s} + \frac{1}{3p_3^2+2rp_3+s}\right).$

For time $t=\tau$ the decay of the top of the pulse when passing through the transformer will be determined by the expression:

$$\Delta = E\left[1 - \frac{1}{L_s C}\left(\frac{1}{3p_1^2 + 2rp_1 + s}e^{p_1\tau} + \right.\right.$$

$$\left.\left. + \frac{1}{3p_2^2+2rp_2+s}e^{p_2\tau} + \frac{1}{3p_3^2+2rp_3+s}e^{p_3\tau}\right)\right]. \quad (11)$$

To determine the main parameters of a rectangular pulse at the output of the transformer, τ_F calculations were made for the decay of top (Δ) for the parameters: $R_1 = 5\ \Omega$; $L_M = 8\cdot10^{-4}$ H; $R_2 = 0{,}1122\cdot10^{-2}\ \Omega$; $K_{Tr} = 66{,}74$:

$$L_S = \mu_{ap} W_1^2 \frac{p_{w1}(\Delta n + \frac{d_1 + d_2}{3})}{l} =$$

$$= 4{,}5\cdot10^{-4}\cdot8^2\,\frac{0{,}08(0{,}03\cdot10^{-3}+0{,}06\cdot10^{-3})}{0{,}04} = 5\cdot10^{-6}\text{H},$$

where:

μ_{ap} – absolute magnetic permeability, $4{,}5\cdot10^{-4}$ H/m;
p_{w1} – the average length of the primary coil is 0,08 m;
Δn – insulation thickness between windings, $0{,}03\cdot10^{-4}$ m;
W_1 – number of turns of the primary winding, 8;
d_1 – diameters of the wire of the transformer primary winding, $0{,}1\cdot10^{-3}$ m;
d_2 – diameters of the wire of the transformer secondary winding, $0{,}08\cdot10^{-3}$ m;
l – winding length along the length of the coil, 0,04 m.

To determine the capacitance of the electrodes of the GDV device's cell, the discriminant D's dependence on the value of the capacitance C was obtained (Fig. 8).

τ_F calculations by formula (10) and top decay by formula (11) showed that the duration of the leading edge was 11,2 ns, and the peak decay (Δ) did not exceed 0,006U.

Based on the volume-weight parameters of the power source, we use the power supply circuit for the GDV generator from capacitive storage (Fig. 9). The main advantage of this method is the highest efficiency of the charging circuit.

The storage capacity charge device is a current stabilizer on a field-effect transistor (Fig. 10).

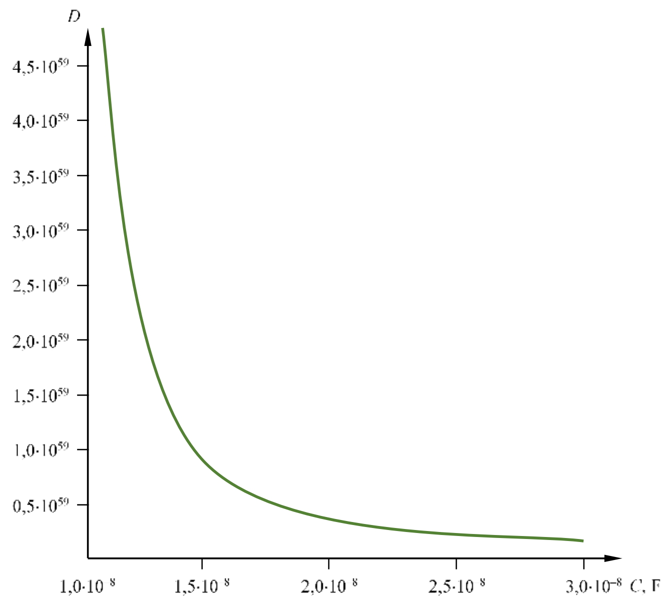

Fig. 8 Discriminant dependence on the capacitance of the electrodes of the cell of the GDV device

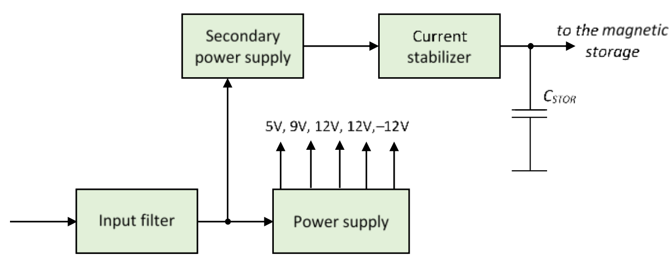

Fig. 9 Functional diagram of the GDV generator power supply

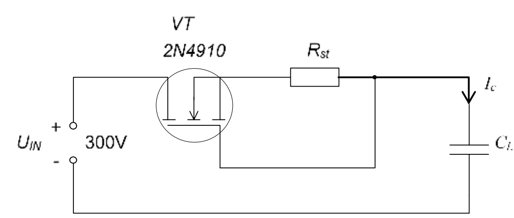

Fig. 10 Electric circuit of the current stabilizer

The required value of the storage capacitor C_{STOR} is determined from the expression:

$$P_{OUT} = \frac{C_{STOR}U^2}{2} f_d, \quad (12)$$

where P_{OUT} is the output power of the power supply; C_{STOR} is the charging capacity, F; U is the voltage on the capacitor, V; f_d is the discharge repetition rate, Hz.

The value of the storage capacity C_{STOR} with its partial discharge is determined from expression (12), given that:

$U^2 = (U_{END} - U_{START})^2$;

$$C_{stor} = \frac{2P_{OUT}}{(U_{END}-U_{START})^2 f_d}. \quad (13)$$

The required time for recharging the capacity from U_{START} to U_{END} is determined through the operation of the A_{SUPP}:

$$A_{SUPP} = \int_0^{T-\tau_d} U_{OUT} i_c dt = \int_0^{T-t_d} U_{OUT} C \frac{dU_c}{dt} = \int_{U_{START}}^{U_{END}} U_{OUT} C, \quad (14)$$

where:

$U_{OUT} = U_{END}$;
U_{START} – voltage on the capacitor at the charge start;
U_{END} – voltage at the end of the charge;
$i_c dt = C\frac{dU_c}{dt}$ – instantaneous value of the charge current;
T – the pulse repetition period, 10^{-5} s;
$\tau_d = \tau$– capacitor discharge time, 10^{-6} s.

Divisioning the right and left parts of equation (14) by T, we obtain an expression for power:

$$P_{OUT} = \frac{U_{OUT} C (U_{END}-U_{START})}{T}. \quad (15)$$

Since we know the time required to recharge the capacitance from (15), we find the value of the storage capacitance:

$$C_{STOR} = \frac{P_{OUT}\tau_c}{U_{OUT}(U_{END}-U_{START})}. \quad (16)$$

The value of the stabilizer current is determined from the expression:

$$I_c = \frac{C_{STOR}(U_{END}-U_{START})}{T}, \quad (17)$$

where I_c is the capacitor charge current.

To determine the output resistance of the current stabilizer, we use the equation:

$$R_{OUT} = \frac{(U_{END}-U_{START})}{I_c}. \quad (18)$$

Numerical analysis to determine the parameters of the device showed that they are equal:

$R_{st} = R_{OUT} = 100\ \Omega$; $C_{STOR} = 0{,}2\ \mu F$; $I_c = 0{,}03$ A.

Calculations were made for parameters: $P_{OUT} = 20$ W; $T=10^{-5}$ s; $U_{OUT} = U_{END} = 300$ V; $U_{END} - U_{START} = 3$ V.

5. Conclusion

1. The pulse generator should be based on the method of accumulating electrical energy in the form of the energy of a magnetic field of inductance, which simultaneously combines the accumulation of energy and an increase in voltage up to 20 kV.
2. Ensuring the level of stabilization of the generator output pulse amplitude is not less than 1% due to the need for a system for the amplitude of the output pulse stabilization usage, according to the principle of comparison with the previous pulse.
3. Quartz frequency stabilization should ensure the stability of the pulse repetition rate and time intervals between pulses in the generators of synchronizing pulses and time intervals.
4. For undistorted transmission of a pulsed signal through a transformer, it is necessary to use the developed method for calculating the design parameters of a transformer (the duration of the leading edge was 11,2 ns, and the decay of the peak (Δ) does not exceed $0{,}006U$. The capacitance of the cell electrodes for GDV biological objects should be within 6…8 pF.
5. The accumulative capacity charge device is a current stabilizer with the following parameters: $R_{st} = R_{OUT} = 100\ \Omega$; $C_{STOR} = 0{,}2\ \mu F$; $I_c = 0{,}03$ A.

References

[1] Kuchin, L. F., Cherenkov, O. D., and Kosulina, N. G., "Using the Kirlian Effect to Monitor the Condition of Bioobjects and the Physical Mechanism of Obtaining These Images," *Wisnik of Kharkiv State Technical University of Silskoe Gospodarstva, Problems of Energy Supply and Energy Saving in the Agricultural Industry of Ukraine, Harkiv: HDTUSG,* no. 10, pp. 116–121, 2002.

[2] Kosulina, N. G., "Analysis of Methods for Reaching the Interaction of an Electromagnetic Field with Biological Objects," *Wisnik of Kharkiv State Technical University of Silskoe Gospodarstva, Problems of Energy Supply and Energy Saving of VAPK in Ukraine, Harkiv: HDTUSG*, vol. 1, no. 19, pp. 202-212, 2003.

[3] Kosulina, N. G., Cherenkov, O. D., and Kuchin, L. F., "Substantiation of the Device for the Study of Biological Objects Based on the Kirlian Effect," *Works. Tavri State Agrotechnical Academy, Melitopol: TDATA,* no. 15, pp. 13–18, 2004.

[4] Kosulina, N. G., and Kosulin, S. V., "Application of Low-Energy Wave Radiation in Medicine and Animal Husbandry," *Application of Low-Energy Radio-Wave Emissions in Medicine and Animal Husbandry, the Scientific Heritage (Budapest, Hungary)*, no. 99, pp. 22-25, 2022. [CrossRef]

[5] Bertalanfi Fon L., *General Systems Theory-A Critical Review*, A Research Book on General Systems Theory, Per S English M., Progress, 1999.

[6] Natalia Kosulina, "Electrophysical Parameters of Materials and Bioobjects, Methods and Means of their Measurement in Electrotechnological Processe," *Sworld Journal,* vol. 1, no. 15, pp. 14–20, 2022. [CrossRef]

[7] Antomonov, Yu. G., *Modeling of Biological Systems,* Handbook, K., Naukova Dumka, 1997.

[8] Adler, Yu. P., Markova, E. V., and Granovskij, Yu. V., *Designing an Experiment in Searching for Optimal Conditions, M., Science*, 2011.

[9] I. N. Bronshtein et al., *Pocket Book of Mathematics*, 6th Edition, Wissenschaftlicher Verlag Harri Deutsch Gmbh, Frankfurt Am Main, with 745 Figures and 142 Tables, 2005.

[10] Vadym Popriadukhin et al., "Analysis of the Electromagnetic Field of Multilayered Biological Objects for their Irradiation in a Waveguide System," *Eastern-European Journal of Enterprise Technologies*, vol. 6, no. 5, pp. 58–65, 2017. [CrossRef]

[11] Igor Konstantinov et al., "Theoretical Analysis of Electromagnetic Field Electric Tension Distribution in the Seeds of Cereals," *Research Journal of Pharmaceutical, Biological and Chemical Sciences*, vol. 6, no. 6, pp. 1686–1694, 2015.

[12] Kosulina, N. G., and Cherenkov, A. D., "Theoretical Analysis of the Formation Processes of the Gas Discharge Image of Bioobjects Based on the Kirlian Effect," *Energy Saving, Energy. Energy Audit, National Research and Production and Information Journal*, vol. 2, no. 60, pp. 21–27, 2009.

[13] Cherenkov, A. D., Pirotti E. L., and Kosulina, N. G., "Effect of Low-Energy EMFs on the Probability of Recombination of Radical Pairs in Biological Objects," *Bulletin of Kharkiv State Polytechnic University, Harkiv: HDPU*, no. 105, pp. 137–140, 2000.

[14] Cherenkov, A. D., Pirotti, E. L., and Kosulina, N. G., "Probability of Recombination of Radical Pairs and Biological Objects Under Resonance Impact of EMF on Them," *Visnyk of Kharkiv State Polytechnic University,, Harkiv: HDPU*, no. 106, pp. 39–42, 2000.

[15] N. G Kosulina et al., "Device for Express Diagnostics of a Biological Object of Plant Origin Using Gas Discharge Imaging (Kirlian Effect)," *Stalemate. 15435 Ukraine, MPK (2006) G03B41/00*, no. 7, p. 3, 2006.

[16] N. G Kosulina et al., "Method for Determining Biotropic Parameters of an Electromagnetic Field Based on the Kirlian Effect for Pre-sowing Treatment of Cereal Crops Seeds)," *Stalemate. 18210 Ukraine, MPK (2006) G03B41/00*, no. 11, p. 4, 2006.

[17] N. G Kosulina et al., "Device for Photographing and Examining Biological Objects Based on the Kirlian Effect)," *Stalemate. 18211 Ukraine, MPK (2006) G03B41/00*, no. 11, p. 4, 2006.

[18] Kosulina N. G., and Cherenkov, A. D., "Methods for Construction of Control Systems for Bioobjects When Exposed to Them by Electromagnetic Fields of the Extremely High-Frequency Range," *East European Journal of Advanced Technologies*, vol. 4/2, no. 22, pp. 35–37, 2006.

[19] Adel S. Sedra, Kenneth C. Smith, and Arun N. Chandorkar, *Microelectronic Circuits: Theory and Applications*, Oxford University Press, 2017.

[20] Bogdan, M. Wilamowski, and J. David Irwin, *Fundamentals of Industrial Electronics*, The Industrial Electronics Handbook Second Edition, Taylor and Francis Group, LLC, 2011.

[21] Kosulina, N. G., "Choice of Current Stabilization Device in Pulse Transformer for Non-Destructive Testing Systems of Bioobjects When Exposed to them by EMP KVh Range," *Tavri State Agrotechnical Academy, Proceedings, Melitopol: TDATA*, no. 43, pp. 43–51, 2006.

[22] Krishtafovich, N. A., "Investigation of Remagnetization Losses in Ring-Shaped Ferromagnetic Cores," *Problems of Converting Technique, Kiev*, pp. 91–93, 1979.

[23] Wes Hayward, Rick Campbell, and Bob Larkin, *Experimental Methods in Rf Design*, Amer Radio Relay League, 2003.

[24] Anil K. Maini, *Digital Electronics Principles, Devices and Applications*, Defence Research and Development Organization (DRDO), India, John Wiley & Sons, 2007.